



Title	Smoking enhances the expression of angiotensin-converting enzyme 2 involved in the efficiency of severe acute respiratory syndrome coronavirus 2 infection
Author(s)	Suzuki, Rigel; Ono, Yuki; Noshita, Koji; Kim, Kwang Su; Ito, Hayato; Morioka, Yuhei; Tamura, Tomokazu; Okuzaki, Daisuke; Tagawa, Tetsuzo; Takenaka, Tomoyoshi; Yoshizumi, Tomoharu; Shimamura, Teppei; Iwami, Shingo; Fukuhara, Takasuke
Citation	Microbiology and immunology, 67(1), 22-31 https://doi.org/10.1111/1348-0421.13034
Issue Date	2023-01
Doc URL	http://hdl.handle.net/2115/91065
Rights	This is the peer reviewed version of the following article: Suzuki, R, Ono, Y, Noshita, K, Kim, KS, Ito, H, Morioka, Y, et al. Smoking enhances the expression of angiotensin-converting enzyme 2 involved in the efficiency of severe acute respiratory syndrome coronavirus 2 infection. Microbiol Immunol. 2023; 67: 22– 31. which has been published in final form at https://doi.org/10.1111/1348-0421.13034 . This article may be used for non-commercial purposes in accordance with Wiley Terms and Conditions for Use of Self-Archived Versions. This article may not be enhanced, enriched or otherwise transformed into a derivative work, without express permission from Wiley or by statutory rights under applicable legislation. Copyright notices must not be removed, obscured or modified. The article must be linked to Wiley 's version of record on Wiley Online Library and any embedding, framing or otherwise making available the article or pages thereof by third parties from platforms, services and websites other than Wiley Online Library must be prohibited.
Type	article (author version)
Additional Information	There are other files related to this item in HUSCAP. Check the above URL.
File Information	Main text final 2 (Revise) .pdf



[Instructions for use](#)

Smoking Enhances the Expression of Angiotensin-Converting Enzyme 2 Involved in the Efficiency of Severe Acute Respiratory Syndrome Coronavirus 2 Infection

Rigel Suzuki^{1,#}, Yuki Ono^{2,#}, Koji Noshita^{3,4,#}, Kwang Su Kim⁵, Hayato Ito¹, Yuhei Morioka¹, Tomokazu Tamura¹, Daisuke Okuzaki⁶, Tetsuzo Tagawa², Tomoyoshi Takenaka², Tomoharu Yoshizumi², Tepei Shimamura⁷, Shingo Iwami^{5,8,9,10,11,12}, and Takasuke Fukuhara^{1,*}

¹Department of Microbiology and Immunology, Graduate School of Medicine, Hokkaido University, Sapporo, 060-8638, Hokkaido, Japan

²Department of Surgery and Science, Graduate School of Medicine, Kyushu University, Fukuoka, 819-0395, Fukuoka, Japan

³Department of Biology, Kyushu University, Fukuoka, 819-0395, Fukuoka, Japan

⁴Plant Frontier Research Center, Kyushu University, Fukuoka, 819-0395, Fukuoka, Japan

⁵Interdisciplinary Biology Laboratory (iBLab), Division of Biological Science, Graduate School of Science, Nagoya University, Nagoya, 464-8602, Aichi, Japan

⁶Genome Information Research Center, Research Institute for Microbial Diseases, Osaka University, Suita, 565-0871, Osaka, Japan

⁷Division of Systems Biology, Graduate School of Medicine, Nagoya University, Nagoya, 464-8602, Aichi, Japan

⁸Institute of Mathematics for Industry, Kyushu University, Fukuoka, 819-0395, Fukuoka, Japan

⁹Institute for the Advanced Study of Human Biology (ASHBi), Kyoto University, Kyoto, 606-8501, Kyoto Japan

¹⁰NEXT-Ganken Program, Japanese Foundation for Cancer Research (JFCR), Koutou, 135-8550, Tokyo, Japan

¹¹Interdisciplinary Theoretical and Mathematical Sciences (iTHEMS), RIKEN, Wako, 351-0198, Saitama, Japan

¹²Science Groove Inc., Fukuoka, 810-0041, Fukuoka, Japan

#These authors contributed equally to this work.

*Corresponding Author: Takasuke Fukuhara

Department of Microbiology and Immunology, Graduate School of Medicine, Hokkaido University, Sapporo, 060-8638, Hokkaido, Japan

Tel: +81-11-706-6905

Fax: +81-11-706-6905

E-mail: fukut@pop.med.hokudai.ac.jp (T.F.)

Funding:

This work was supported by the Ministry of Health, Labour and Welfare of Japan and the Japan Agency for Medical Research and Development (JP21fk018471h0001, JP20fk0108451h0001, JP21nf0101627h0002, JP21fk0108617h0001, JP20fk0108401h0001 and JP21wm0325004h0002 to T.F.), the Japan Society for the Promotion of Science KAKENHI (JP21H02736 to T.F. and JP20K22951, JP21K15452 to R.S.), JST MIRAI Program (JPMJMI20G6 to K.N.), and Moonshot R&D (JPMJMS2021 to S.I. and JPMJMS2025 to S.I.).

Acknowledgments:

We thank H. Kubo and K. Tsushima for their secretarial work, W. Noguchi, K. Oyama, N. Tachibana, T. Matuoka and M. Honmura for their technical assistance. We also thank Edanz (<https://jp.edanz.com/ac>) for editing a draft of this manuscript.

Conflicts of Interest:

The authors declare that there are no competing commercial or financial interests.

Institutional Review Board Statement:

This study has been approved by the institutional review board of Kyushu University (approval no. 2020-807).

Informed Consent Statement:

This study is retrospective study. Enrolled patients were not required to give informed consent to this study because the analysis used specimens acquired from surgery. We applied opt-out method on this study by announcing this research on website of Kyushu University.

Data Availability Statement:

Data sharing is not applicable to this article.

57
58
59
60
61
62
63
64
65
66
67
68
69
70
71
72
73
74
75
76
77
78
79
80
81
82
83
84
85
86
87
88
89
90
91
92
93
94
95
96
97
98
99
100
101
102
103
104
105
106
107
108
109

Co-authors:

- Rigel Suzuki, rigels@pop.med.hokudai.ac.jp
Yuki Ono, i.l.b.o.c.0704@gmail.com
Koji Noshita, noshita@morphometrics.jp
Kwang Su Kim, kwangsu815@gmail.com
Hayato Ito, ito.hayato.c4@elms.hokudai.ac.jp
Yuhei Morioka, ym6831@icloud.com
Tomokazu Tamura, tomokazu.tamura@pop.med.hokudai.ac.jp
Daisuke Okuzaki, dokuzaki@biken.osaka-u.ac.jp
Tetsuzo Tagawa, t_tagawa@surg2.med.kyushu-u.ac.jp
Tomoyoshi Takenaka, takenaka.tomoyoshi@gmail.com
Tomoharu Yoshizumi, yoshizumi.tomoharu.717@m.kyushu-u.ac.jp
Teppei Shimamura, shimamura@med.nagoya-u.ac.jp
Shingo Iwami, iwamishingo@gmail.com
Takasuke Fukuhara, fukut@pop.med.hokudai.ac.jp

110 **Abstract**

111 Smoking is one of the risk factors most closely related to the severity of COVID-19. However, the
112 relationship between smoking history and SARS-CoV-2 infectivity is unknown. In this study, we evaluated
113 the *ACE2* expression level in the lungs of current smokers, ex-smokers, and non-smokers. The *ACE2*
114 expression level of ex-smokers who smoked cigarettes until recently (cessation period shorter than 6 months)
115 was higher than that of non-smokers and ex-smokers with a long history of non-smoking (cessation period
116 longer than 6 months). We also showed that the efficiency of SARS-CoV-2 infection was enhanced in a
117 manner dependent on the *ACE2* expression level. Using RNA-seq analysis on the lungs of smokers, we
118 identified that the expression of inflammatory signaling genes was correlated with *ACE2* expression. Notably,
119 with increasing duration of smoking cessation among ex-smokers, not only *ACE2* expression level but also
120 the expression levels of inflammatory signaling genes decreased. These results indicated that smoking
121 enhances the expression levels of *ACE2* and inflammatory signaling genes. Our data suggest that the
122 efficiency of SARS-CoV-2 infection is enhanced by smoking-mediated upregulation of *ACE2* expression
123 level.

124

125 **Keywords:** ACE2; COVID-19; inflammation; SARS-CoV-2; smoking.

126

127 **Abbreviations:** ACE2, angiotensin-converting enzyme 2; COVID-19, coronavirus disease 2019; SARS-
128 CoV-2, Severe acute respiratory syndrome coronavirus 2; TCID₅₀, 50% tissue culture infective doses;
129 TMPRSS2, transmembrane protease serine 2; COPD, chronic obstructive pulmonary disease;

130

131

132

133

134

135

136

137

138

139

140

141

142

143

144

145

146

147

148

149

150

151

152

153

154

155

156

157

158

159

160

161

162

163

164

165

166

167

168 **1. Introduction**

169 Severe acute respiratory syndrome coronavirus 2 (SARS-CoV-2) in the genus *Betacoronavirus* in the
170 family Coronaviridae is the causative agent of the global pandemic of severe respiratory disease, coronavirus
171 disease 2019 (COVID-19) ¹. The virus was initially discovered in Wuhan, China, in late December 2019 ^{2,4}
172 and has spread worldwide. As of August, 8, 2022, more than 585 million COVID-19 cases have been
173 confirmed in over 180 countries, and more than six million deaths have been reported
174 (<https://covid19.who.int/>).

175 To enter host cells, SARS coronavirus binds its spike protein to a host cell receptor, ACE2 (angiotensin-
176 converting enzyme 2); a recent study has also reported that SARS-CoV-2 uses ACE2 for cell entry ⁵.
177 Moreover, the spike protein needs to be activated and cleaved by host cell enzyme proteases such as
178 transmembrane protease serine 2 (TMPRSS2) and FURIN ^{6,7}. Upon examining plasma ACE2 during
179 hospitalization due to COVID-19, elevated baseline plasma ACE2 in COVID-19 patients was significantly
180 associated with increased disease severity during the hospitalization period ⁸. Therefore, ACE2 would be a
181 risk factor for a more serious COVID-19 presentation, and the levels of the above-mentioned proteins
182 involved in the infectious pathway should have significant implications for clinical outcomes. Identifying the
183 background of populations with high expression of the *ACE2* gene may be important not only for public
184 health but also for prevention and treatment of COVID-19.

185 Smoking is one of the risk factors for respiratory infectious disorders, including viral infections ⁹.
186 Inflammatory cells infiltrate into the mucosa and glandular tissue due to smoke exposure, which leads to the
187 excessive production of mucus. This has additional harmful effects, such as epithelial-cell hyperplasia,
188 prevention of tissue repair, thickened small bronchioles, and emphysema ¹⁰. A previous investigation reported
189 that a significantly higher proportion of patients with a history of smoking exhibited a rapid deterioration in
190 health during their admission for COVID-19 compared with non-smokers (27% versus 3%, $p = 0.018$),
191 suggesting that smoking may have a harmful effect on COVID-19 prognosis ¹¹. Moreover, smoking history
192 was found to be associated with a severe condition of COVID-19 among young adults ¹², and a meta-analysis
193 revealed that smoking is a risk factor for the progression of COVID-19, with smokers having 1.91 times the
194 odds of deteriorating COVID-19 severity than never-smokers ¹³. Biologically, cigarette smoking reportedly
195 increases the expression of ACE2 in the lower airways ¹⁴. Although smoking has been confirmed to confer a
196 risk of severe COVID-19, the relationship between smoking history and SARS-CoV-2 infectivity is unknown.

197 In this study, we evaluated the association between smoking history and the *ACE2* expression of lung
198 tissue. We revealed a correlation between the period of smoking cessation and the expression of *ACE2*.
199 Virological and mathematical analyses showed that ACE2 expression level is important for the efficiency of
200 SARS-CoV-2 infection. In addition, RNA-seq analysis showed that the expression of inflammatory signaling
201 genes also correlates with the period of smoking cessation and *ACE2* expression level. These results suggest
202 that smoking upregulates the *ACE2* expression level that is involved in the efficiency of SARS-CoV-2
203 infection.

204
205
206
207
208
209
210
211
212
213
214
215
216
217
218
219
220
221
222
223
224
225

226 **2. Materials and Methods**

227 *2.1. Lung tissue sample collection and RT-qPCR*

228 Lung tissue was obtained from patients who underwent surgery at the Department of Surgery and Science,
229 Graduate School of Medical Sciences, Kyushu University, between January 2013 and December 2019.
230 Clinicopathological features were examined: sex, blood type, smoking history, and respiratory disease
231 [chronic obstructive pulmonary disease (COPD) or interstitial pneumonia (IP)]. If the period of smoking
232 cessation before surgery was less than 6 months, this was categorized into 1-month intervals. Patients who
233 still smoked or who had a cessation period shorter than 6 months were defined as current smokers, while
234 patients with a cessation period longer than 6 months were defined as ex-smokers. Clinical information and
235 follow-up data were obtained from the patients' medical records. Tissue samples were immediately flash-
236 frozen in liquid nitrogen after resection and stored at -80°C until the preparation of cDNA from RNA
237 extracted from the samples. Total RNA of lung tissue was extracted using ISOGEN (Nippon Gene Co., Ltd.,
238 Tokyo, Japan, #315-02504). The concentration of total RNA was measured using a DS-11 Series
239 Spectrophotometer (DeNovix, Wilmington, USA). Total RNA (1 μg) was reverse-transcribed into cDNA
240 using Super Script III First-Strand Synthesis Super Mix (Invitrogen, Thermo Fisher Scientific, Inc.,
241 Massachusetts, USA, #11752050), in accordance with the manufacturer's protocol. qPCR was performed
242 with Applied Biosystems StepOnePlus real-time PCR system (Life Technologies, California, USA). TaqMan
243 gene expression assays (Applied Biosystems, Massachusetts, USA) for *ACE2* (Hs00965485_g1), *TMPRSS2*
244 (Hs01122322_m1), and *FURIN* (Hs00965485_g1) were used, while *GAPDH* (Hs01122322_m1) was used
245 as an internal control. Relative expression of *ACE2*, *TMPRSS2*, and *FURIN* was calculated using the $\Delta\Delta\text{CT}$
246 method. This study was approved by Kyushu University Institutional Review Board for Clinical Research
247 (2020-807).

248

249 *2.2. Statistical analysis and normalization*

250 All assays were performed independently at least two times. The data were summarized in box plots. The
251 statistical significance of associations of *ACE2*, *TMPRSS2*, and *FURIN* expression levels with clinical
252 background factors was tested by the Mann–Whitney *U*-test. The trend for changes of *ACE2* expression
253 levels with increasing duration of smoking cessation was tested by the Jonckheere–Terpstra test.

254

255 *2.3. Cells*

256 *TMPRSS2*-expressing Vero E6 (VeroE6/*TMPRSS2*) cells were obtained from the Japanese Collection of
257 Research Bioresources Cell Bank (JCRB1819) and maintained in low-glucose Dulbecco's Modified Eagle's
258 Medium (low-glucose DMEM) (Sigma-Aldrich, St. Louis, USA, #D6046) containing 10% fetal bovine
259 serum (FBS) (Biowest, Bradenton, France, #S1810) and G418 (Nacalai Tesque, Kyoto, Japan, #09380-44).
260 The HEK293-3P6C33 (HEK293/tet-*ACE2*) cells¹⁵ were a gift from Dr. Matsuura at Osaka University, and
261 maintained in high-glucose Dulbecco's Modified Eagle's Medium (Nacalai Tesque, #08459-35) containing
262 10% FBS and blasticidin (solution) (10 $\mu\text{g}/\text{ml}$) (Invivogen, California, USA, #ant-bl-1), and the exogenous
263 expression of *ACE2* and *TMPRSS2* was induced by the addition of doxycycline hydrochloride (1 $\mu\text{g}/\text{ml}$)
264 (Sigma-Aldrich, #D5207). All of the above cells were cultured at 37°C under 5% CO_2 .

265

266 *2.4. Plasmids*

267 Full-length cDNAs for *TMPRSS2* were amplified by PCR from a cDNA library derived from HEK293/tet-
268 *ACE2* cells. The PCR fragment was cloned into the pCSII-EF-based vector with a C-terminal HA tag. This
269 expression vector was used for experiments after verification of the sequence of inserted DNA.

270

271 *2.5. SARS-CoV-2 preparation and titration*

272 B.1.1 (GISAID ID: EPI_ISL_408667), B.1.1.7 variant (GISAID ID: EPI_ISL_804007), B.1.351 variant
273 (GISAID ID: EPI_ISL_1122890), and P.1 variant (GISAID ID: EPI_ISL_833366) were obtained from the
274 National Institute of Infectious Diseases. All viruses were amplified in VeroE6/*TMPRSS2* cells and the
275 culture supernatants were harvested and stored at -80°C until use. The infectious titers in the culture
276 supernatants were determined by the 50% tissue culture infective doses (TCID_{50}). The culture supernatants
277 of cells were inoculated onto VeroE6/*TMPRSS2* cells in 96-well plates after 10-fold serial dilution with
278 DMEM containing 2% FBS, and the infectious titers were determined at 72 h post-infection (hpi). All
279 experiments involving SARS-CoV-2 were performed in biosafety level-3 laboratories, following standard
280 biosafety protocols approved by Hokkaido University.

281

282 *2.6. SARS-CoV-2 infection*

283 HEK293/tet-*ACE2* cells (200,000 cells) treated with 0.05–1000 ng/ml doxycycline for 24 h were seeded

284 into a 12-well plate. One day prior to infection, TMPRSS2-HA was transfected into the cells with Trans IT
285 LT-1 (Mirus, Wisconsin, USA, #MIR2306), following the manufacturer's protocol. Twenty-four hours later,
286 SARS-CoV-2 was inoculated and incubated at 37°C for 1 h. The cells were washed and new culture medium
287 was added. After 18~19 h of incubation, the infected cells were harvested and subjected to western blotting
288 and RT-qPCR.

289

290 2.7. Human lung tissue extracts

291 Human lung tissue (~10 mg) was ground using BioMasher II (Nippi, Tokyo, Japan, #320203) in RIPA
292 buffer containing 50 mM Tris-HCL pH 7.6, 150 mM NaCl, 1% TritonX-100, 0.5% sodium deoxycholate,
293 0.1% SDS, 1 mM EDTA, 10 mM NaF, and 25 μM MG-132. The lysates were kept on ice for 30 min and
294 sonicated using Bioruptor® II (Sonicbio Co., Ltd., Nagoya, Japan). After centrifugation at 10,000 g for 20
295 min at 4°C, the supernatants were mixed with SDS sample buffer (Bio-Rad, California, USA, #1610737).

296

297 2.8. Western blotting

298 Whole-cell lysates or the lung extracts were subjected to SDS-PAGE and transferred onto polyvinylidene
299 fluoride transfer membranes (Millipore, Massachusetts, USA, #IPVH00010). The membranes were then
300 immunoblotted with specific antibodies as indicated and subsequently incubated with horseradish
301 peroxidase-conjugated antibody against mouse or rabbit immunoglobulin (Jackson ImmunoResearch
302 Laboratories, Pennsylvania, USA, #115-0035-003 and #111-035-003), followed by detection with ECL
303 western blotting detection reagents (Cytiva, Massachusetts, USA, #RPN2106). The following antibodies
304 were used in this study: anti-SARS-CoV Nucleoprotein (Sino Biological, Beijing, China, #40143-MM05),
305 anti-ACE2 (Proteintech, Rosemont, USA, #21115-1-AP), anti-GAPDH (Wako, Osaka, Japan, #NBP2-
306 27103H) and anti-HA (BioLegend, SanDiego, USA, #902301).

307

308 2.9. RT-qPCR from cell

309 Total RNA was extracted from the SARS-CoV-2-infected cells using a RNeasy Mini Kit (QIAGEN,
310 #74104). The sample was used as the template for RT-qPCR performed in accordance with the manufacturer's
311 protocol using the One Step PrimeScript™ III RT-qPCR Mix (Takara, #RR600B) and the following primers
312 and probe: Forward, 5'-CAC ATT GGC ACC CGC AAT C-3'; Reverse, 5'-GAG GAA CGA GAA GAG GCT
313 TG-3'; Probe, FAM-ACT TCC TCA AGG AAC AAC ATT GCC A-BHQ. These primers target the
314 *nucleocapsid* gene of SARS-CoV-2. Fluorescent signals were acquired using a StepOnePlus™ Real Time
315 PCR System (Applied Biosystems).

316

317 2.10. Quantifying viral RNA corresponding to ACE2 expression level

318 We evaluated the dependence of viral RNA replication on *ACE2* expression using the Hill function:

$$319 \quad V = \frac{1}{1 + \left(\frac{A}{EC_{50}}\right)^{-m}}, \quad (1)$$

320 where V is the amount of viral RNA normalized by the maximum viral RNA for each strain, A is the *ACE2*
321 expression level, EC_{50} is the *ACE2* expression level that achieves 50% of maximum expressed viral RNA,
322 and m is the Hill coefficient (corresponding to the steepness of the curve). We used the least-squares
323 regression approach to fit Eq. (1) to viral RNA data and estimated the values of EC_{50} and m .

324

325 2.11. Non-negative matrix factorization

326 To extract representative patterns of expression profiles and investigate the relationship between these
327 patterns and clinical background, we used non-negative matrix factorization (NMF) for RNA-seq data of 23
328 normal lung tissues. We first selected the top 8,000 genes ranked by variance in read counts. In NMF, for the
329 given expression matrix X for 23 samples and 8,000 genes, we sought matrices W and H such that

$$330 \quad X \approx WH$$

331 where W is a $23 \times k$ contribution matrix, H is a $k \times 8,000$ excitation matrix, and k is the number
332 of factors. NMF generates factors with significantly reduced dimensions compared with the original matrix.
333 The key property of NMF is that W and H are constrained to be positive matrices. The (n, l) -element
334 $w_{n,l}$ of matrix W can be interpreted as the contribution to factor l of sample n , and the (l, k) -element
335 $h_{l,k}$ of matrix H can be interpreted as the relative abundance of the k -th gene given factor l . In our analysis,
336 W and H are estimated using a variational Bayesian inference¹⁶ and the number of factors was selected by
337 the evidence lower bound (ELBO).

338

339 *2.12. Pathway enrichment analysis*

340 To identify key pathways that are related to each factor in NMF, pathway enrichment analysis using
341 Fisher's exact test was performed on the top 500 genes for each factor ranked by coefficients, as supplied by
342 columns of W . The gene lists of 321 pre-annotated pathways collected from KEGG
343 (<http://www.genome.jp/kegg/>) were used for enrichment analysis and pathways with a p-value $< 10^{-5}$ were
344 selected as significant.

345
346
347
348
349
350
351
352
353
354
355
356
357
358
359
360
361
362
363
364
365
366
367
368
369
370
371
372
373
374
375
376
377
378
379
380
381
382
383
384
385
386
387
388
389
390
391
392
393
394
395
396

3. Results

3.1. *ACE2* expression level is associated with smoking

To investigate the associations of *ACE2*, *TMPRSS2*, and *FURIN* expression with clinical background, we analyzed the expression levels of these genes by RT-qPCR using normal human lung tissues. We tested *ACE2* (Hs00965485_g1, Applied Biosystems), *TMPRSS2* (Hs01122322_m1, Applied Biosystems), *FURIN* (Hs00965485_g1, Applied Biosystems), and *GAPDH* (Hs01122322_m1, Applied Biosystems) expression levels, and it was confirmed that the expression of these target genes could be measured by the $\Delta\Delta\text{CT}$ method. Samples with a *GAPDH* CT value less than 28 were included in this analysis. Finally, 245 patients whose normal lung tissues were sampled from 2013 to 2018 were enrolled in this study. The expression level of *ACE2* was not associated with other clinical background factors apart from smoking and COPD/IP. However, the *ACE2* expression of smokers was significantly higher than that of non-smokers ($p=0.00272$) (Figure 1A), while the *ACE2* expression of current smokers was higher than that of ex-smokers ($p=0.00011$, Figure 1B), which was consistent with previous results¹⁷. Moreover, the expression showed a statistically significant decrease with increasing duration of smoking cessation ($p<0.0001$, Figure 1C and Figure S1). Of the 184 patients with a history of smoking, one patient was excluded because the duration of smoking cessation was unknown. Our results demonstrated that current smokers had higher expression of *ACE2* than ex-smokers and the long period of smoking cessation might decrease *ACE2* expression in normal lung tissue. Meanwhile, *TMPRSS2* and *FURIN* expression was not associated with clinical factors, including smoking status, except for *FURIN* expression differing between females and males (Figure 1D and 1E). These results indicate that *ACE2* may be the protein that is most associated with smoking.

3.2. *ACE2* expression level is important for the efficiency of SARS-CoV-2 infection

Although *ACE2* is a receptor for SARS-CoV-2 infection, it is not yet clear to what extent *ACE2* expression levels affect virus propagation. To clarify whether differences of *ACE2* expression levels affect the infectivity of SARS-CoV-2, SARS-CoV-2 infectivity to HEK293 cells expressing *ACE2* at various levels was examined. First, we established HEK293 cells in which *ACE2* expression could be induced with doxycycline (HEK293/tet-*ACE2*)¹⁵. Moreover, HA-tagged *TMPRSS2* was expressed in HEK293/tet-*ACE2* cells (Figure S2). The expression levels of *ACE2* depended on the concentration of doxycycline added to the supernatant of HEK293/tet-*ACE2*. At 1 day after treatment with tetracycline, D614G-bearing B.1.1 isolate (GISAID ID: EPI_ISL_408667), B.1.1.7 variant (GISAID ID: EPI_ISL_804007), B.1.351 variant (GISAID ID: EPI_ISL_1122890), and P.1 variant (GISAID ID: EPI_ISL_833366) were used to infect HEK293 cells expressing *ACE2* at various levels. As the expression level of *ACE2* increased, N protein levels in the cells were increased (Figure 2A). Moreover, viral RNA in the cells were also increased in a manner dependent on the level of *ACE2* expression (Figure 2B). These results suggest that high expression of *ACE2* contributes to the efficient propagation of SARS-CoV-2. Interestingly, low expression of *ACE2* facilitated replication of B.1.1.7, B.1.351, and P.1 variants, compared with that of the B.1.1 isolate, suggesting that the spike protein of the variants can bind *ACE2* more efficiently than that of B.1.1 (Figure 2B). Many reports have shown that N501Y in these variants enhances the efficiency of binding between spike protein and *ACE2*¹⁸⁻²⁰. To confirm that the expression level of *ACE2* in normal human lung tissue falls within the range of *ACE2* protein levels induced by doxycycline, we quantified the *ACE2* protein levels of six human lung tissues. *ACE2* expression was normalized using *GAPDH*. We found that the normalized *ACE2* expression level was 0.330–0.769 in human lung tissues (Figure 2C). As shown in Fig. 2A, the expression level of *ACE2* protein induced by doxycycline was 0.072–1.759, indicating that the *ACE2* expression level in the doxycycline-treated cells included the range of that in human lung tissue. Next, to further clarify the effect of *ACE2* expression level on the replication of SARS-CoV-2, we first quantified the maximum level of viral RNA for each strain: P.1 variants showed a higher level of viral RNA (9.2×10^6) than the other variants (B.1.1.7: 6.0×10^6 , B.1.1: 3.7×10^6 , B.1.1.7: 2.5×10^6). To evaluate the dependence of viral RNA replication on *ACE2* expression, we normalized the viral RNA by its maximum level (Figure 2D) and fitted the Hill function [see Eq. (1) in Materials and Methods for details]. Compared with other variants, we found that the B.1.1 isolate showed the highest EC_{50} and the lowest m (Figure 2E). This implies that B.1.1.7, B.1.351, and P.1 variants replicate their viral RNA more efficiently than the B.1.1 isolate at the same *ACE2* expression level.

3.3. Identification of pathways involved in *ACE2* expression in human lung

To identify representative patterns of gene expression profiles in human normal lung tissues and to investigate the association between *ACE2* expression and clinical background, we performed non-negative matrix factorization on the gene expression matrix of 23 normal lung tissue samples and 8,000 genes. Six representative factors were selected to maximize the evidence lower bound (ELBO), and their contributions to each sample are shown in Figure 3a. Among the six factors, factors 3 and 4 were significantly correlated

455 with *ACE2* expression (Figure 3B). Pearson's correlation coefficients of factors 3 and 4 for *ACE2* were 0.546
456 and 0.608, and their significance levels were $p=0.0071$ and $p=0.0021$, respectively. We also found that the
457 scores of factors 3 and 4 tended to be higher with a shorter duration of smoking cessation (Figure 3C).
458 Furthermore, we investigated pathways enriched in relation to factors 3 and 4 using Fisher's exact test (Figure
459 3D). We showed that factor 4 was associated with immune-related pathways such as TNF signaling and IL-
460 17 signaling, and infectious disease-related pathways such as human papillomavirus, Kaposi sarcoma-
461 associated herpesvirus, salmonella, human cytomegalovirus, influenza A, and malaria. Among the six
462 representative patterns of gene expression profiles, the results summarized that two were related to *ACE2*
463 expression and the duration of smoking cessation, and one was associated with immunity- and infection-
464 related molecular pathways.

465
466
467
468
469
470
471
472
473
474
475
476
477
478
479
480
481
482
483
484
485
486
487
488
489
490
491
492
493
494
495
496
497
498
499
500
501
502
503
504
505
506
507
508
509
510
511
512

4. Discussion

Smoking is considered to be one of the risk factors for severe COVID-19. Indeed, smoking has been reported to increase the mortality rate and severity of COVID-19²¹. The WHO has also indicated that smoking is a factor in the severity of SARS-CoV-2 infections. However, despite the clear involvement of smoking in SARS-CoV-2 infection, many unanswered questions remain regarding how the extent and duration of smoking affect SARS-CoV-2 infection. In this study, we found that the expression level of *ACE2* was significantly increased in smokers (Figure 1A). In addition, the *ACE2* expression of current smokers was higher than that of ex-smokers (Figure 1D). Meanwhile, we found no differences of *TMPRSS2* and *FURIN* expression levels between smokers and non-smokers (Figure 1B and C). These results suggest that smoking enhances the efficiency of SARS-CoV-2 infection through increased expression of *ACE2*. In fact, the efficiency of SARS-CoV-2 infection increased in a manner dependent on the level of *ACE2* expression (Figure 2A and B). Moreover, as a result of mathematical analysis of the dependence of viral RNA replication on *ACE2* expression, we found that B.1.1.7, B.1.351, and P.1 variants tended to propagate more efficiently than B.1.1 at the same *ACE2* expression level (Figure 2D and E). This could indicate one of the reasons why B.1.1.7, B.1.351, and P.1 variants spread more rapidly throughout the world. In addition, we identified two groups of genes that correlate with *ACE2* expression using RNA-seq (Figure 3A and B). The duration of smoking cessation as well as *ACE2* expression was associated with the upregulation of Factor 4, which is related to inflammation (Figure 3C). Although the genes comprising Factor 3 have various functions, the genes of Factor 4 are associated with inflammatory signaling (Figure 3D). These results suggest that there is a relationship between *ACE2* expression and inflammatory signaling.

Many papers have reported on the association between smoking and *ACE2* expression^{14,17,22-28}. Some papers also reported that nicotine downregulates the expression level of *ACE2* in certain tissues and cell types^{23-25,27}. However, in this study, we observed that the *ACE2* expression level was upregulated in current smokers. This discrepancy may have been due to the use of nicotine in previous studies. Tobacco contains many chemical substances, so substances other than nicotine may be involved in inflammation and *ACE2* expression. Smith et al. reported that the *ACE2* expression level is upregulated in lung tissue of COPD patients as well as smokers. Consistent with this report, we showed that not only smoking but also COPD increased *ACE2* expression levels in the lung. In several reports, COPD was identified as a risk factor for severe COVID-19²⁹. Therefore, COPD may also enhance the efficiency of SARS-CoV-2 infection and the severity of COVID-19 via increased expression of *ACE2*.

To understand the mechanism behind the effects of upregulated *ACE2*, we performed transcriptomic analysis to identify the gene expression patterns correlated with *ACE2* expression (Figure 3B). Factor 4 contains multiple pathways related to immune response, suggesting that *ACE2* expression is influenced by immune response. In fact, one study has reported that INF- α , INF- β , and INF- γ treatment increased *ACE2* expression in tracheal cells¹⁷. Moreover, cigarette smoke is an inflammatory substance and smokers tend to exhibit increases in inflammatory markers^{17,30,31}. These findings suggest that inflammatory signaling induced by smoking is associated with the upregulation of *ACE2*. In the current study, we showed that the *ACE2* expression level of current smokers was higher than that of ex-smokers (Figure 1D). Moreover, with increasing duration of smoking cessation, the *ACE2* expression level was downregulated (Figure 1E). These results may indicate that the *ACE2* expression level decreases due to the alleviation of lung inflammation resulting from smoking cessation.

A variety of SARS-CoV-2 variants have been found globally. Among them, the WHO defined B.1.1.7, B.1.351, and P.1 as variants of concern, and named them alpha, beta, and gamma strains, respectively. The spike proteins of these variants have the N501Y mutation in common. It has been reported that the presence of this mutation may increase the efficiency of infection due to enhanced binding to *ACE2*³². In this study, the infectivity of SARS-CoV-2 was enhanced in a manner dependent on *ACE2* expression, and the infection ratios were efficiently established in these mutations at the same *ACE2* expression level compared to the conventional strain (Figure 2A and B). The current data support the finding that N501Y mutation increases the binding of *ACE2* to the spike protein of SARS-CoV-2. However, because clinical isolates were used in this study and other mutations may increase the efficiency of infection, detailed analysis using recombinant SARS-CoV-2 with N501Y mutation will be needed in the future.

In summary, we provide evidence that the expression levels of *ACE2* and inflammatory signaling genes are elevated in the lungs of current smokers and ex-smokers with a short period of smoking cessation. Moreover, increased *ACE2* expression level is associated with elevated infectivity of SARS-CoV-2. These findings suggest that smoking history may be associated with the infectivity of SARS-CoV-2. An interesting challenge for the future will be to determine the detailed molecular pathway behind the upregulation of *ACE2* induced by smoking and inflammation.

571 **Figure legends**

572 **Figure 1.**

573 **Expression of *ACE2*, *TMPRSS2*, and *Furin* in human lung tissues**

574 Box plots of gene expression of (A) *ACE2*, (D) *TMPRSS2*, and (E) *FURIN* in normal lung tissue in association
575 with clinical factors. The expression levels of *ACE2* were significantly different between smokers and non-
576 smokers (Mann–Whitney *U*-test, $p=0.00272$), and between non-COPD/IP and COPD/IP sufferers (Mann–
577 Whitney *U*-test, $p=0.00342$). No significant difference was found in the expression levels of *TMPRSS2*. The
578 expression level of *FURIN* was significantly different between women and men (Mann–Whitney *U*-test,
579 $p=0.00496$). (B) A box plot of the expression of *ACE2* among smokers. The expression level was significantly
580 higher in current smokers (cessation period shorter than 6 months) than in former smokers (cessation period
581 longer than 6 months); Mann–Whitney *U*-test, $p = 0.00011$. (C) A box plot of the expression of *ACE2* with
582 the period of smoking cessation. The expression of *ACE2* tended to decrease with increasing duration of
583 smoking cessation. Jonckheere–Terpstra test, $p < 0.0001$.

584

585 **Figure 2.**

586 ***ACE2* expression level is important for the efficiency of SARS-CoV-2 infection**

587 (A) Dependence of the infection efficiency of SARS-CoV-2 on the expression level of *ACE2*. HEK293/tet-
588 *ACE2* cells were transfected with HA-tagged *TMPRSS2*. After 24h of transfection, *TMPRSS2* expressing
589 HEK293/tet-*ACE2* cells were treated with various concentrations of doxycycline for 24 h. The cells were
590 infected with SARS-CoV-2 (MOI=1). After 18 h of infection, the cell lysate was blotted with anti-*ACE2*,
591 anti-N, anti-HA, and anti-GAPDH antibodies. (B) Involvement of *ACE2* expression in the infection of
592 various SARS-CoV-2 variants. HEK293/tet-*ACE2* cells expressing HA-tagged *TMPRSS2* with doxycycline
593 treatment were infected with SARS-CoV-2 variants (MOI=1). After 19 h of infection, RNA was isolated from
594 the cells and viral RNA was quantified by RT-PCR. The amount of viral RNA was normalized by dividing
595 by the amount of minimum viral RNA in the doxycycline treatment or non-treatment. (C) The expression
596 level of *ACE2* in human lung tissue. The lysates from eight human normal lungs were blotted with anti-
597 *ACE2* and anti-GAPDH antibodies. Lower numbers represent the expression level of *ACE2* normalized by
598 the expression level of GAPDH. (D) The closed dots and solid line correspond to the observed data and the
599 best-fit solution for Eq. (1). (E) Estimated values of EC_{50} and m are shown.

600

601 **Figure 3.**

602 **Relationships between six factors identified by non-negative matrix factorization and *ACE2* expression,
603 duration of smoking cessation, and pathways**

604 (A) Heatmap of the 23×6 contribution matrix H estimated by non-negative matrix factorization and *ACE2*
605 expression. The six factors were selected to maximize the ELBO. Each row represents the contribution of
606 the six factors for each sample. (B) Scatter plots of the third and fourth factor scores (x-axis) and *ACE2*
607 expression (y-axis). The line represents the prediction line for linear model fitting, and the filled colors
608 represent the confidence interval. (C) Boxplots of the third and fourth factor scores for non-smokers and
609 smokers with three durations of smoking cessation (> 6 months, 1 month to < 6 months, and < 1 month). (D)
610 Significantly enriched pathways of the third and fourth factors. The x-axis represents $-\log_{10}(p\text{-value})$ of
611 Fisher’s exact test, while the y-axis represents the pathway name.

612

613

614

615

616

617

618

619

620

621

622

623

624

625

626

627

628

629 **Author Contributions:**
630 Conceptualization, Y.O., K.N., T.S., S.I., and T.F. Funding acquisition, R.S., K.N., S.I., and T.F.
631 Methodology, R.S., Y.O., K.N., K.K., Y.M., D.O., T.S., S.I., and T.F. Investigation, R.S., Y.O., K.N., K.K.,
632 Y.M., H.I., T.T. (Tamura), D.O., T.T. (Tagawa), T.T. (Takenaka), T.Y. T.S., S.I., and T.F. Data curation,
633 R.S., Y.O., K.N., T.S., S.I., and T.F. Writing—original draft preparation, R.S., Y.O., K.N., T.S., S.I., and
634 T.F. Writing—review and editing, R.S., Y.O., K.N., K.K., Y.M., D.O., T.S., S.I., and T.F. Supervision, T.F.
635 All authors have read and agreed to the published version of the manuscript.

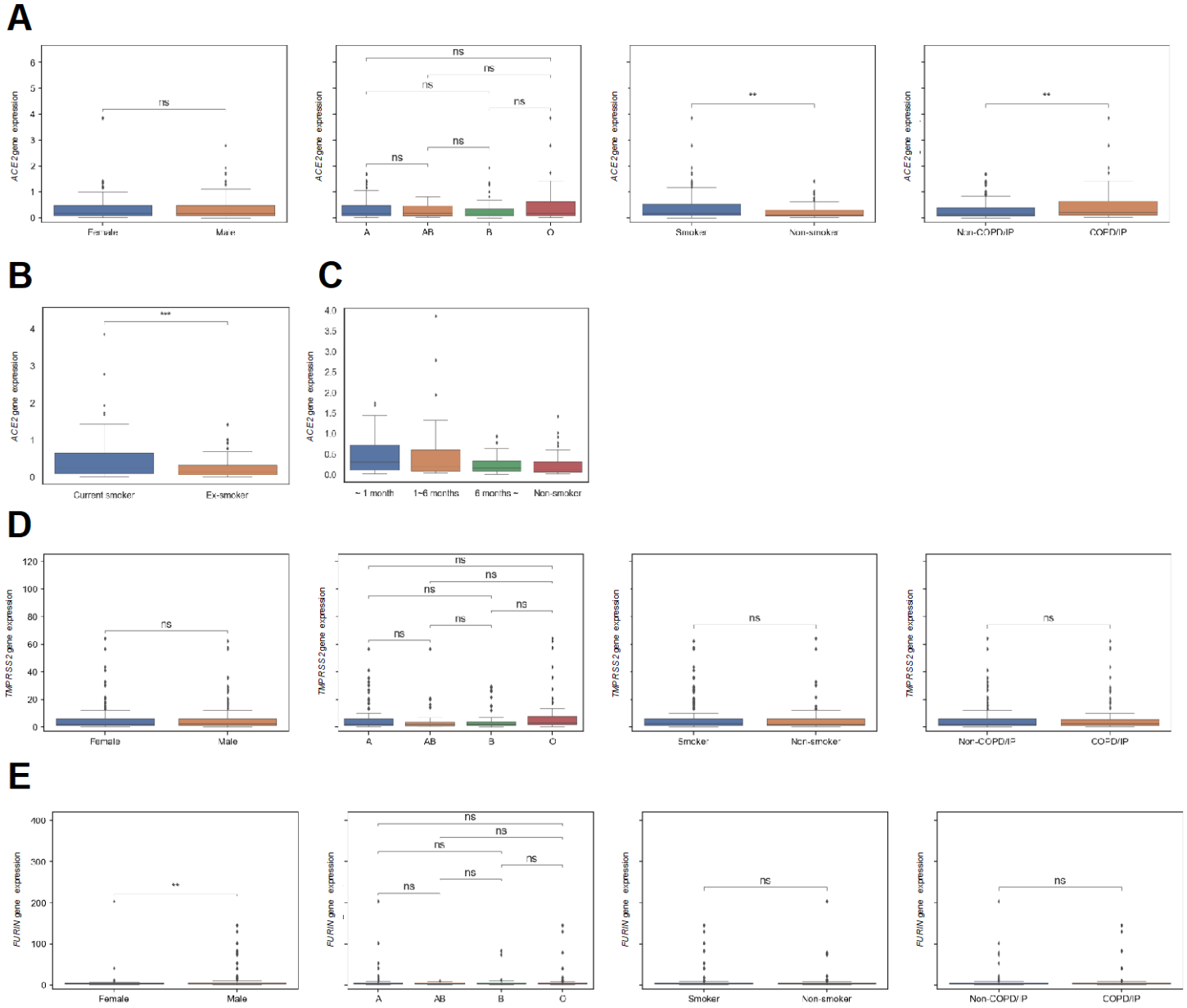
636
637
638
639
640
641
642
643
644
645
646
647
648
649
650
651
652
653
654
655
656
657
658
659
660
661
662
663
664
665
666
667
668
669
670
671
672
673
674
675
676
677
678
679
680
681
682
683
684
685
686

687 **References**

- 688 1. Gorbalenya AE, Baker SC, Baric RS, et al. The species Severe acute respiratory syndrome-
689 related coronavirus: classifying 2019-nCoV and naming it SARS-CoV-2. *Nat Microbiol.*
690 2020;5(4):536-544.
- 691 2. Zhu N, Zhang D, Wang W, et al. A Novel Coronavirus from Patients with Pneumonia in China,
692 2019. *N Engl J Med.* 2020;382(8):727-733.
- 693 3. Zou L, Ruan F, Huang M, et al. SARS-CoV-2 Viral Load in Upper Respiratory Specimens of
694 Infected Patients. *N Engl J Med.* 2020;382(12):1177-1179.
- 695 4. Wu F, Zhao S, Yu B, et al. A new coronavirus associated with human respiratory disease in
696 China. *Nature.* 2020;579(7798):265-269.
- 697 5. Zhou P, Yang XL, Wang XG, et al. A pneumonia outbreak associated with a new coronavirus of
698 probable bat origin. *Nature.* 2020;579(7798):270-273.
- 699 6. Hoffmann M, Kleine-Weber H, Schroeder S, et al. SARS-CoV-2 Cell Entry Depends on ACE2
700 and TMPRSS2 and Is Blocked by a Clinically Proven Protease Inhibitor. *Cell.* 2020;181(2):271-
701 280.e278.
- 702 7. Coutard B, Valle C, de Lamballerie X, Canard B, Seidah NG, Decroly E. The spike glycoprotein
703 of the new coronavirus 2019-nCoV contains a furin-like cleavage site absent in CoV of the same
704 clade. *Antiviral Res.* 2020;176:104742.
- 705 8. Kragstrup TW, Singh HS, Grundberg I, et al. Plasma ACE2 predicts outcome of COVID-19 in
706 hospitalized patients. *PLoS One.* 2021;16(6):e0252799.
- 707 9. Gozdek M, Zieliński K, Pasierski M, et al. Transcatheter Aortic Valve Replacement with Self-
708 Expandable ACURATE neo as compared to Balloon-Expandable SAPIEN 3 in Patients with
709 Severe Aortic Stenosis: Meta-analysis of Randomized and Propensity-Matched Studies. *J Clin*
710 *Med.* 2020;9(3).
- 711 10. MacNee W. Pathophysiology of cor pulmonale in chronic obstructive pulmonary disease. Part
712 One. *Am J Respir Crit Care Med.* 1994;150(3):833-852.
- 713 11. Liu W, Tao ZW, Wang L, et al. Analysis of factors associated with disease outcomes in
714 hospitalized patients with 2019 novel coronavirus disease. *Chin Med J (Engl).*
715 2020;133(9):1032-1038.
- 716 12. Adams SH, Park MJ, Schaub JP, Brindis CD, Irwin CE. Medical Vulnerability of Young Adults to
717 Severe COVID-19 Illness-Data From the National Health Interview Survey. *J Adolesc Health.*
718 2020;67(3):362-368.
- 719 13. Patanavanich R, Glantz SA. Smoking Is Associated With COVID-19 Progression: A Meta-
720 analysis. *Nicotine Tob Res.* 2020;22(9):1653-1656.
- 721 14. Leung JM, Yang CX, Tam A, et al. ACE-2 expression in the small airway epithelia of smokers
722 and COPD patients: implications for COVID-19. *Eur Respir J.* 2020;55(5).
- 723 15. Torii S, Ono C, Suzuki R, et al. Establishment of a reverse genetics system for SARS-CoV-2
724 using circular polymerase extension reaction. *Cell Rep.* 2021;35(3):109014.
- 725 16. Cemgil AT. Bayesian inference for nonnegative matrix factorisation models. *Comput Intell*
726 *Neurosci.* 2009:785152.
- 727 17. Smith JC, Sausville EL, Girish V, et al. Cigarette Smoke Exposure and Inflammatory Signaling
728 Increase the Expression of the SARS-CoV-2 Receptor ACE2 in the Respiratory Tract. *Dev Cell.*
729 2020;53(5):514-529.e513.

- 730 18. Tian F, Tong B, Sun L, et al. N501Y mutation of spike protein in SARS-CoV-2 strengthens its
731 binding to receptor ACE2. *Elife*. 2021;10.
- 732 19. Luan B, Wang H, Huynh T. Enhanced binding of the N501Y-mutated SARS-CoV-2 spike protein
733 to the human ACE2 receptor: insights from molecular dynamics simulations. *FEBS Lett*.
734 2021;595(10):1454-1461.
- 735 20. Zhu X, Mannar D, Srivastava SS, et al. Cryo-electron microscopy structures of the N501Y
736 SARS-CoV-2 spike protein in complex with ACE2 and 2 potent neutralizing antibodies. *PLoS*
737 *Biol*. 2021;19(4):e3001237.
- 738 21. Guan WJ, Ni ZY, Hu Y, et al. Clinical Characteristics of Coronavirus Disease 2019 in China. *N*
739 *Engl J Med*. 2020;382(18):1708-1720.
- 740 22. Brake SJ, Barnsley K, Lu W, McAlinden KD, Eapen MS, Sohal SS. Smoking Upregulates
741 Angiotensin-Converting Enzyme-2 Receptor: A Potential Adhesion Site for Novel Coronavirus
742 SARS-CoV-2 (Covid-19). *J Clin Med*. 2020;9(3).
- 743 23. Ferrari MF, Raizada MK, Fior-Chadi DR. Nicotine modulates the renin-angiotensin system of
744 cultured neurons and glial cells from cardiovascular brain areas of Wistar Kyoto and
745 spontaneously hypertensive rats. *J Mol Neurosci*. 2007;33(3):284-293.
- 746 24. Ferrari MF, Raizada MK, Fior-Chadi DR. Differential regulation of the renin-angiotensin system
747 by nicotine in WKY and SHR glia. *J Mol Neurosci*. 2008;35(2):151-160.
- 748 25. Oakes JM, Fuchs RM, Gardner JD, Lazartigues E, Yue X. Nicotine and the renin-angiotensin
749 system. *Am J Physiol Regul Integr Comp Physiol*. 2018;315(5):R895-R906.
- 750 26. Yilin Z, Yandong N, Faguang J. Role of angiotensin-converting enzyme (ACE) and ACE2 in a
751 rat model of smoke inhalation induced acute respiratory distress syndrome. *Burns*.
752 2015;41(7):1468-1477.
- 753 27. Yue X, Basting TM, Flanagan TW, et al. Nicotine Downregulates the Compensatory
754 Angiotensin-Converting Enzyme 2/Angiotensin Type 2 Receptor of the Renin –
755 Angiotensin System. *Annals ATS*. 2018;15:S126-S127.
- 756 28. Cai G. Tobacco-use disparity in gene expression of ACE2, the receptor of 2019-nCov. 2020;
757 <https://www.preprints.org/manuscript/202002.0051/v1>.
- 758 29. Lippi G, Henry BM. Chronic obstructive pulmonary disease is associated with severe
759 coronavirus disease 2019 (COVID-19). *Respir Med*. 2020;167:105941.
- 760 30. Arnson Y, Shoenfeld Y, Amital H. Effects of tobacco smoke on immunity, inflammation and
761 autoimmunity. *J Autoimmun*. 2010;34(3):J258-265.
- 762 31. Gan WQ, Man SF, Sin DD. The interactions between cigarette smoking and reduced lung
763 function on systemic inflammation. *Chest*. 2005;127(2):558-564.
- 764 32. Starr TN, Greaney AJ, Hilton SK, et al. Deep Mutational Scanning of SARS-CoV-2 Receptor
765 Binding Domain Reveals Constraints on Folding and ACE2 Binding. *Cell*. 2020;182(5):1295-
766 1310.e1220.
767
768

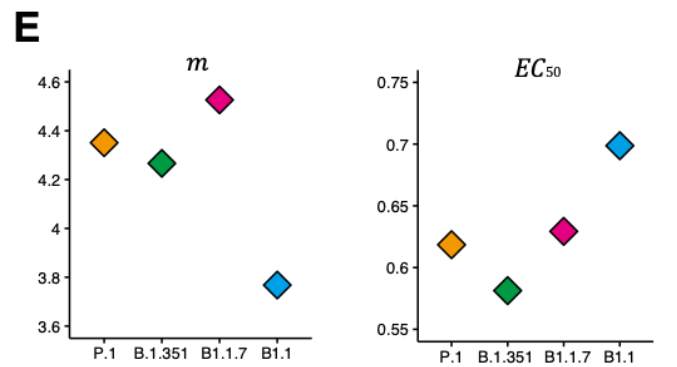
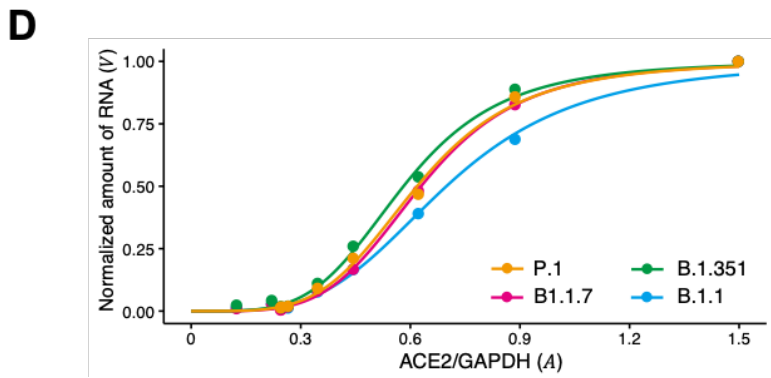
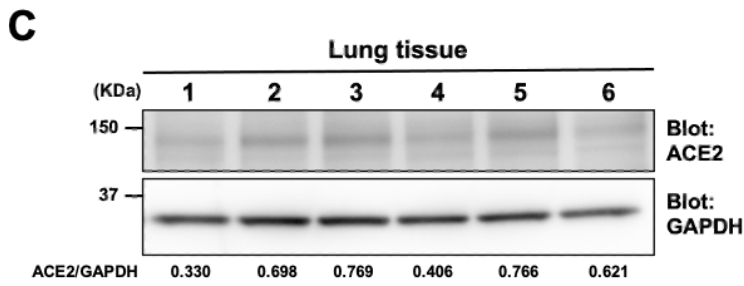
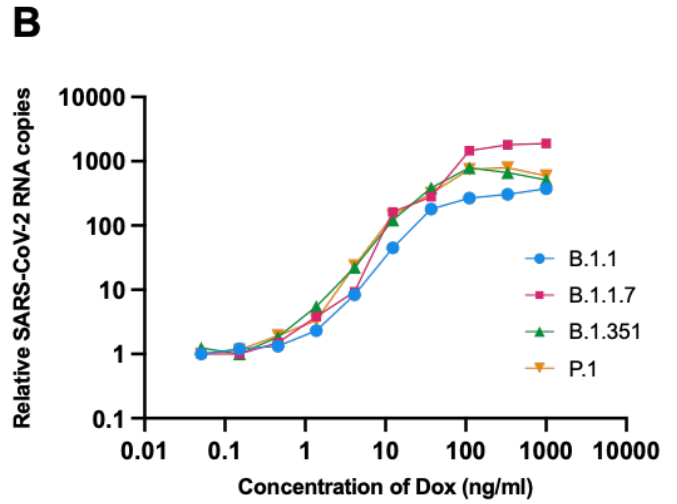
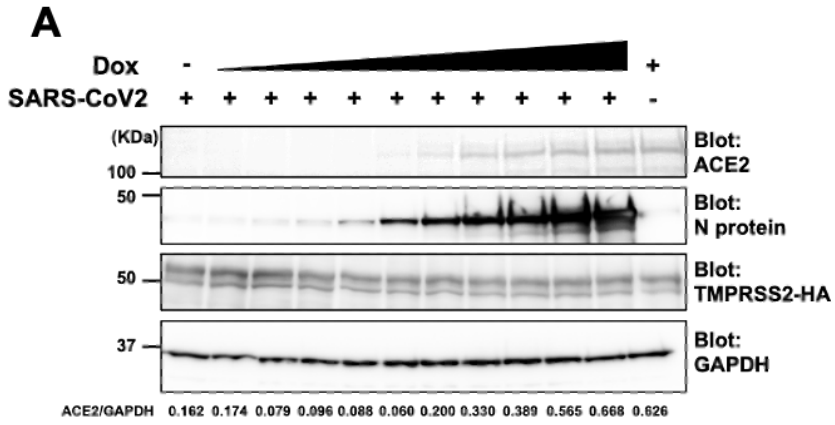
1
2
3
4
5



6
7
8
9
10
11
12
13
14
15
16
17
18
19

Figure.1 Suzuki et. al

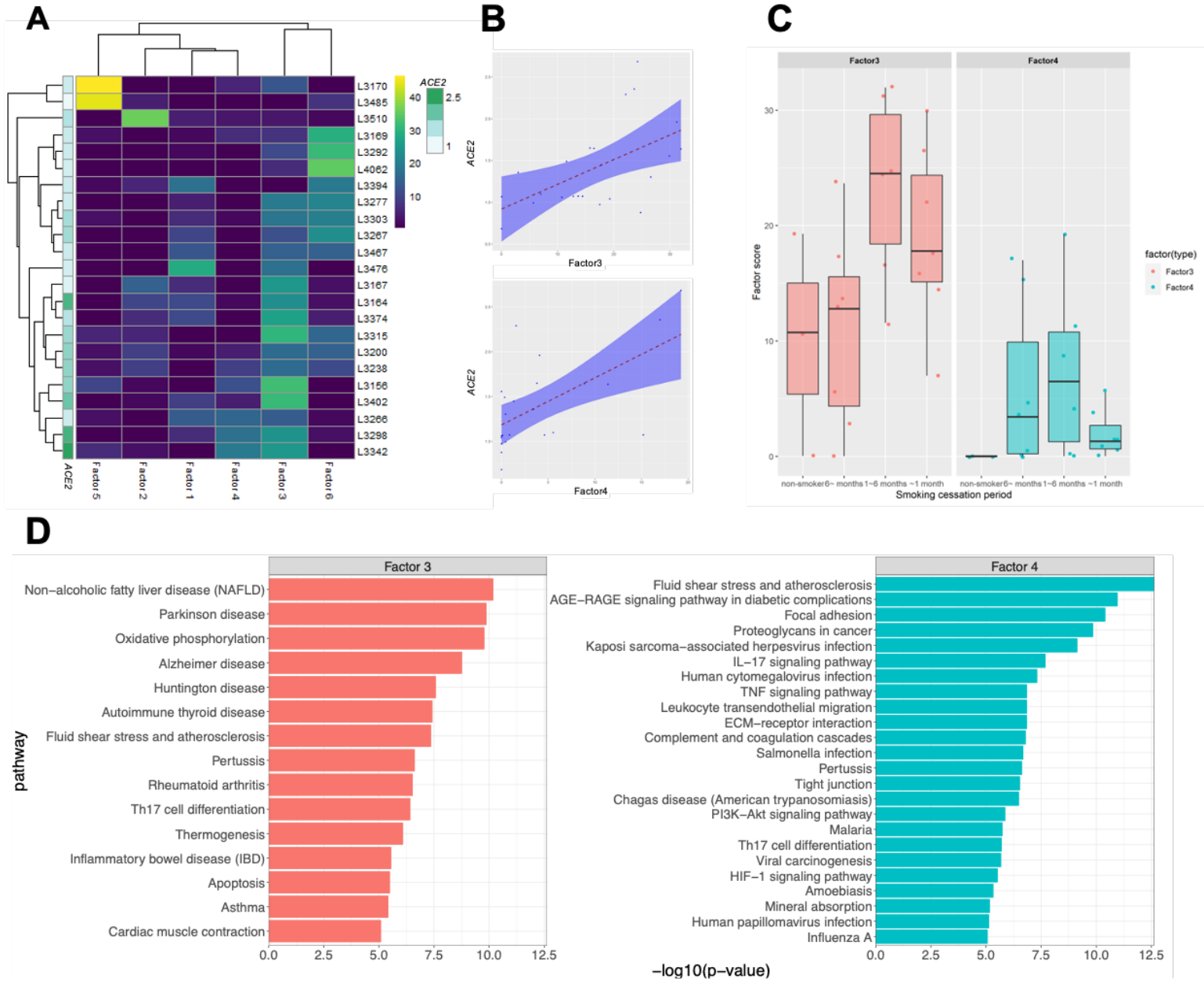
20
21
22
23
24



25
26
27
28
29
30
31
32
33
34
35
36
37
38
39
40
41

Figure.2 Suzuki et. al

42
43



44
45
46
47
48
49
50
51
52
53
54
55
56
57
58
59

Figure.3 Suzuki et. al